Available online at www.sciencedirect.com

ScienceDirect

Procedia Manufacturing 12 (2017) 230 – 241

Procedia MANUFACTURING

International Conference on Sustainable and Intelligent Manufacturing, RESIM 2016, 14-17 December 2016, Leiria, Portugal

Morphology Development During Micro Injection Moulding of Thermoplastics

Geoffrey R Mitchell[a]*, Pedro Carreira[a], Sara Gomes[a], Artur Mateus[a], and Saeed Mohan[b]

[a]*Centre for Rapid and Sustainable Product Development, Institute Polytechnic of Leiria, Rua de Portugal, Marinha Grande, 2430-028, Portugal*
[b]*Department of Chemistry, University of Reading, Whiteknights, RG6 6AD, UK*

Abstract

Micro injection moulding is a key process in the field of micro manufacturing especially in the production of medical devices. Micro injection molding technology involves the injection of the whole material with the result of a high degree of efficiency due to the material saving process. In comparison with conventional large injection moulding, the volume of material is very much reduced and as a consequence the flow and temperature profiles are considerable different to macro injection moulding. This work focuses on the impact on the structure, morphology and properties of parts prepared using micro injection moulding of these changes flow and temperature profiles. We have used small-angle X-ray Scattering techniques to evaluate the semicrystalline morphology and we have discovered that the nature of the process has led to changes in the morphology. We have supplemented the small angle scattering technique with wide-angle x-ray scattering as well differential scanning calorimetry.

Peer-review under responsibility of the scientific committee of the International Conference on Sustainable and Intelligent Manufacturing

Keywords: Micromoulding; medical devices; morphology; properties; semi-crystalline.

* Corresponding author. Tel.: +0-000-000-0000 ; fax: +0-000-000-0000 .
E-mail address: author@institute.xxx

Peer-review under responsibility of the scientific committee of the International Conference on Sustainable and Intelligent Manufacturing
doi:10.1016/j.promfg.2017.08.027

1. Introduction

Micro injection moulding is a key process in the field of micro manufacturing especially in the production of medical devices [1-5]. Micro injection molding technology involves the injection of the whole material with the result of a high degree of efficiency due to the material saving process. In comparison with conventional large injection moulding, the volume of material is very much reduced and as a consequence the flow and temperature profiles are considerable different to macro injection moulding [6]. This work focuses on the impact on the structure, morphology and properties of parts prepared using micro injection moulding of these changes flow and temperature profiles. We anticipate that the substantial changes in the cooling profile will lead to significant changes in the morphology [6].

2. Experimental

2.1 Materials

Moulded specimens for testing were prepared using poly(ε-caprolactone) (PCL) supplied by Perstorp (Capa 6500) with a melt flow index of 7.9-5.9 g/10min-1 and a reported molecular weight of 50,000 (Daltons). It was supplied in the form of 3 mm pellets.

2.2 Micromoulding

Moulded samples were prepared using a BOY 22A Injection Moulding system equipped with Alpha Control. The mould was machined from steel (Figures 1 & 2). The mould had a single feed at the specimen moulds were distributed equidistance from the feed. The mould provided 8 samples of dimensions 10mm x 20mm with differing thicknesses (Table 1).

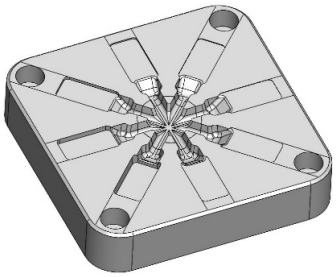

Fig 1: CAD view of one part of the micromould used in this work

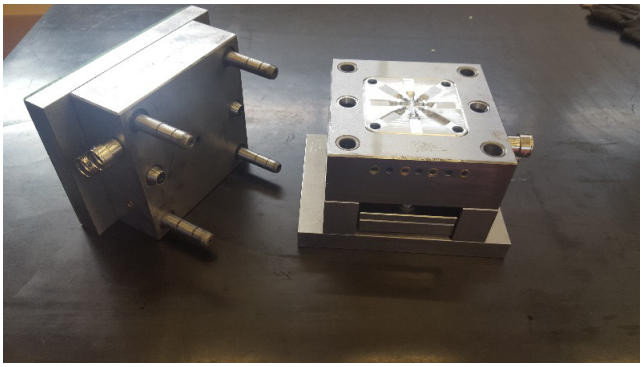

Fig 2 : The complete micromould used in this work

2.3 Differential Scanning Calorimetry (DSC)

Thermal analysis was performed using a Thermal Analysis instrument DSC Q2000 with a heating and cooling rate of 5°C/min. and a sample mass of 2.50 mg – 7 mg was used.

2.4 X-Ray Scattering Measurements

Small angle x-ray scattering (SAXS) and wide angle x-ray scattering (WAXS) experiments were performed on the Bruker AXS Nanostar in the University of Reading Chemical Analysis Facility, UK. The equipment has a compact 3 pin hole collimation and a beam diameter of 0.8 mm. SAXS and WAXS data were collected simultaneously with the small angle data collected on to a 2D 2048 x 2048 pixel frame detector approximately 66 cm distance from the sample. 2D WAXS patterns were collected onto an image plate placed approximately 10 cm from the sample position. A hole in the centre of the WAXS image plate allows for the simultaneous collection of SAXS data. Data was collected from $Q = 0.015$ Å^{-1} – 5 Å^{-1} where $Q = 4\pi\sin\theta/\lambda$, λ is the wavelength and 2θ is the scattering angle. A wavelength of 1.5418 Å was employed. Sample data was collected for 16 - 20 minutes. For calibration of SAXS data a silver behenate standard was used and a corundum standard was used for WAXS calibrations to obtain the sample to detector distance using the known Q values of the diffraction rings of these standards.

2.5 Simulations

Numerical simulations of the mould filling and temperature of the mould walls during the cycle were performed using Moldflow Insight. The corresponding model mesh is represented in Figure 3, with 271937 tetrahedral elements. The characteristic size of each element was 0.9mm. A melt temperature of 63ºC and a mould temperature of 27ºC were considered to simulate the cooling of the plastic.

3. Results

3.1 Simulations

We were able to simulate the cooling of the plastic part inside the micromoulding after filling at 110ºC. The image shown in Figure 3a shows the part which was simulated and the mesh employed in those simulations. For each part we used the simulation to predict the temperature cycle at the mould wall. Figure 3b shows the time taken for the mould wall to call to the crystallization temperature of the PCL plotted as a function of the thickness of each part. As expected the cooling time increases in a parabolic manner with increasing thickness.

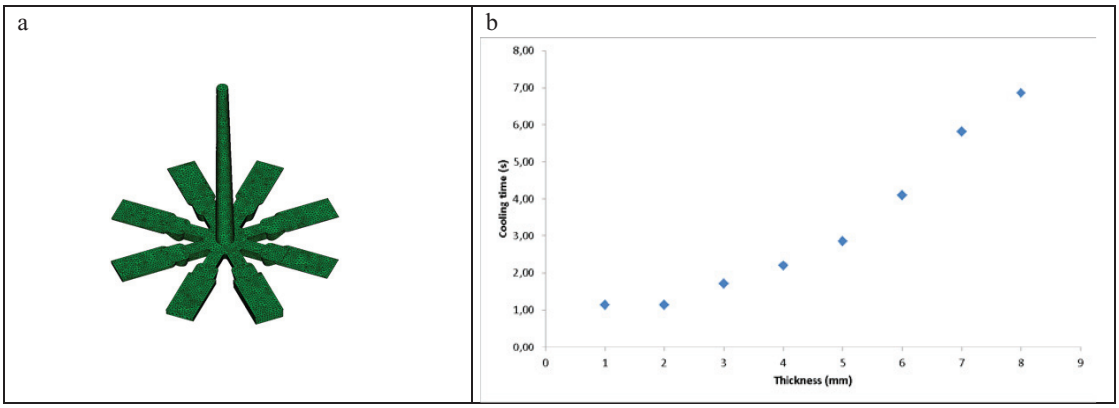

Fig 3 (a) A computer representation of the part which is simulated showing the mesh used in the simulations. (b) a plot of the time taken for the mould wall to cool to the crystallisation temperature of the PCL after the fill cycle for each part as a function of the thickness of that part

3.2 Moulding

Samples were successfully prepared using the following parameters: Injection Temperature: 110 ºC; Injection Pressure:155 bar; Clamp Force: 180 kN. The samples produced had the thicknesses shown in Table 1.

Table 1: Sample thicknesses obtained using the micromould shown in Figure 1

Sample	Thickness (mm)
MM1	0.127
MM2	0.162
MM3	0.226
MM4	0.412
MM5	0.717
MM6	1.179
MM7	2.008
MM8	3.625

3.3 Characteristics of the moulded parts

Small samples were taken from each moulded part in approximately the same location and subjected to analysis using differential scanning calorimetry. The first heating run for each sample was used to measure the level of crystallinity in the sample and to look at the melting behavior. The first run heating curve for sample MM8 is shown in figure 4. This curve is typical for a semi-crystalline polymer sample such as PCL. By measuring the area under the heating curve and scaling using the heat of fusion for a perfectly crystalline system we can obtain the crystallinity values which are shown in Figure 5. We used a value of 139.5 J/g for the heat of fusion for a perfectly crystalline sample [7]

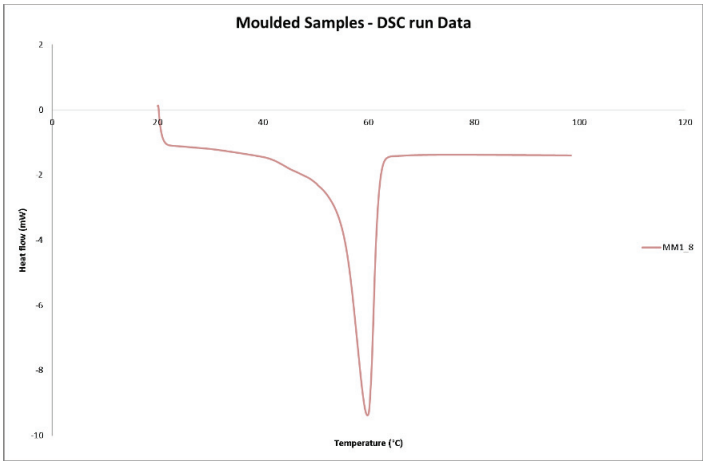

Fig 4: The DSC curve on first heating for the sample MM8.

We can see that the calculated crystallinity for the thinnest micromouldings is the lowest at ~61% but this rises as the moulding thickness increases to a peak value of ~63% for a thickness of 1.17mm and then drops as thicker samples are considered.

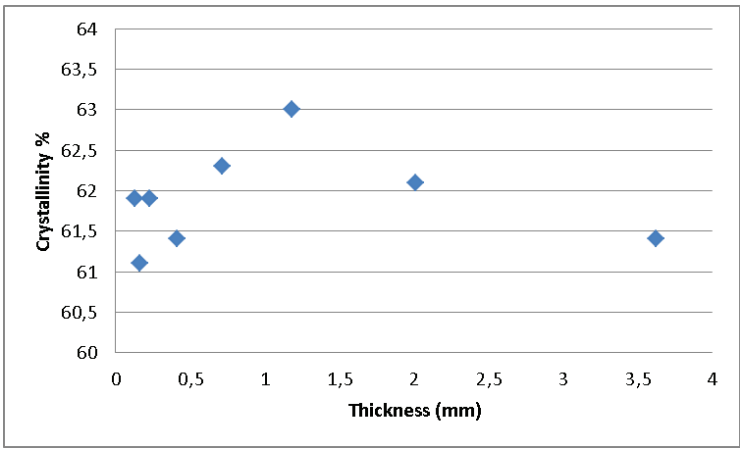

Fig 5: A plot of the calculated crystallinity as a function of the moulded part thickness obtained from the differential scanning calorimetry data.

The characteristics of the melting peak recorded in the DSC are shown in Figure 6. The melt peak value of ~ 57ºC is observed for the thinnest samples and this increases to a value just over 59ºC for a moulding thickness of 1.17mm. The temperature of the peak in the DSC curve is more or less unchanged for thicker samples. A similar trend is observed for the melt onset temperature but this reduces as the mould thickness increases. In this type of mould it is quite likely thata the rate of cooling of the molten polymer as it first impacts on the mould wall is to solidify the material, forming a skin while the subsequent melt material is insulated from the mould and follows through and crystallises later. This processes has been reported for both conventional injection moulding and for micro injection moulding. Clearly any measurement of the orientation using x-ray scattering will average over the

thickness of the sample. We might expect to see different parts of the sample which have crystallised with a different history for example fast cool on the surface but slower cooled on the interior of the sample. Semi-crystalline polymers typically exhibit a broad melting curve in the DSC as a consequence of different thicknesses of lamellar crystals and partly as a consequence of reorganization during heating [reference 6 chapter 2]. In the case of micromoulding these effects are enhanced and some of the characteristics of such morphologies may be seen in the SAXS patterns shown in Figure 8. We might expect to see a highly oriented skin with a second component of an isotropic distribution of chain folded lamellae. The highly oriented parts arises from the templating effect of row nuclei formed from chains stretched out in the flow field. Whether we see the effects of such row nuclei depends on the number formed in the flow field and the relaxation time of the molecular chains as they relax towards an isotropic trajectory. Figure 8.1 shows a highly anisotropic pattern sumperimposed on a level of isotropic scattering. Figure 8.2 shows a much weaker anisotropic pattern which nevertheless is as highly oriented, as judged by the extent of the arcing Figure 8.3 shows a lower level of anisotropy and Figure 8.4 the anisotropic part is more less lost. To observe the anisotropy the crystallization must take place in the presence of the unrelaxaed row nuclei and this means fast cooling which in turn results in thin lamellae and a lower level of crystallinity. Inspection of the simulated cooling times shown in Figure 3b, suggests that the relaxation time of the extended chains the melt must be less than 2s but longer thsn ~1s in line with suggestion made previously that the longest relaxation time for PCL is of the order of a few seconds [9]. As the effective cooling rate slows the lamellae thicken and we observed a rise in the peak melting temperature as well as an increase in the crystallinity. The change in the Melt Onset temperature with the micromoulded part thickness (Figure 6) reflects the changing distribution of lamellae thicknesses as a consequence of the skin/core morphology described above.

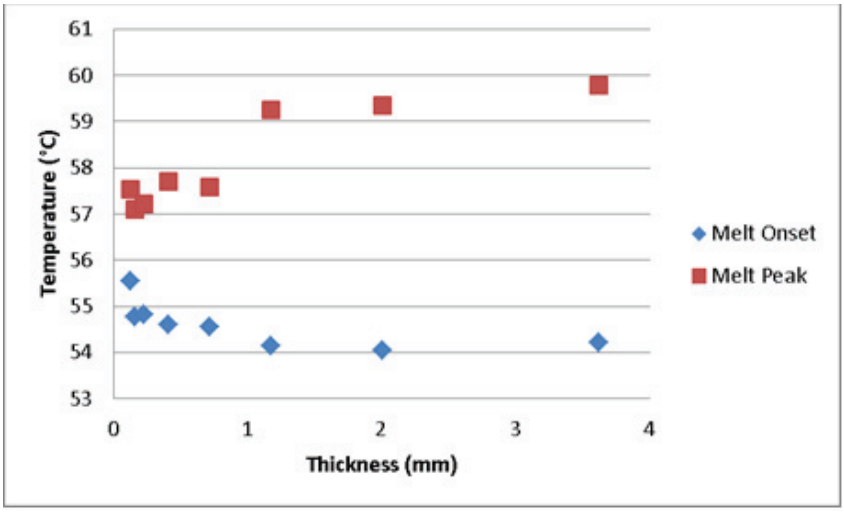

Fig 6: A plot of the melt onset and melt peak as a function of the moulded part thickness obtained from the differential scanning calorimetry data.

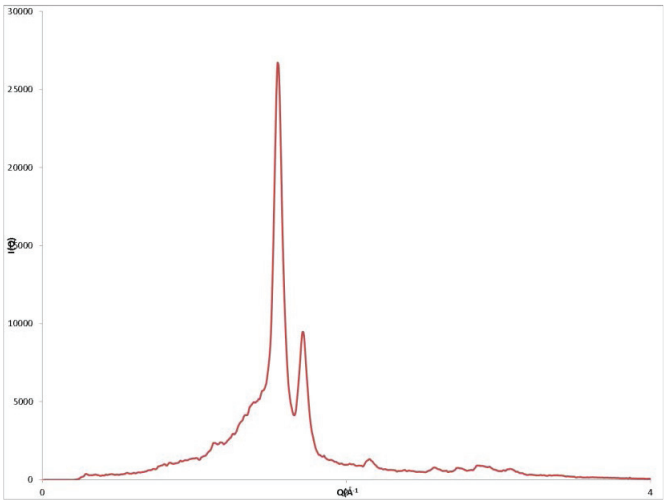

Fig 7: A plot of the WAXS data as a function of the scattering vector Q for the micromoulded sample MM1.

The semi-crystalline nature of the micromoulded samples is confirmed by WAXS analysis. The scattering curve for sample MM1 is shown in Figure 7. The curve is typical of that recorded for PCL samples and each of the micromolded samples shows the same curve which shows that the crystal structure of the PCL is unchanged as a consequence of the micromoulding process.

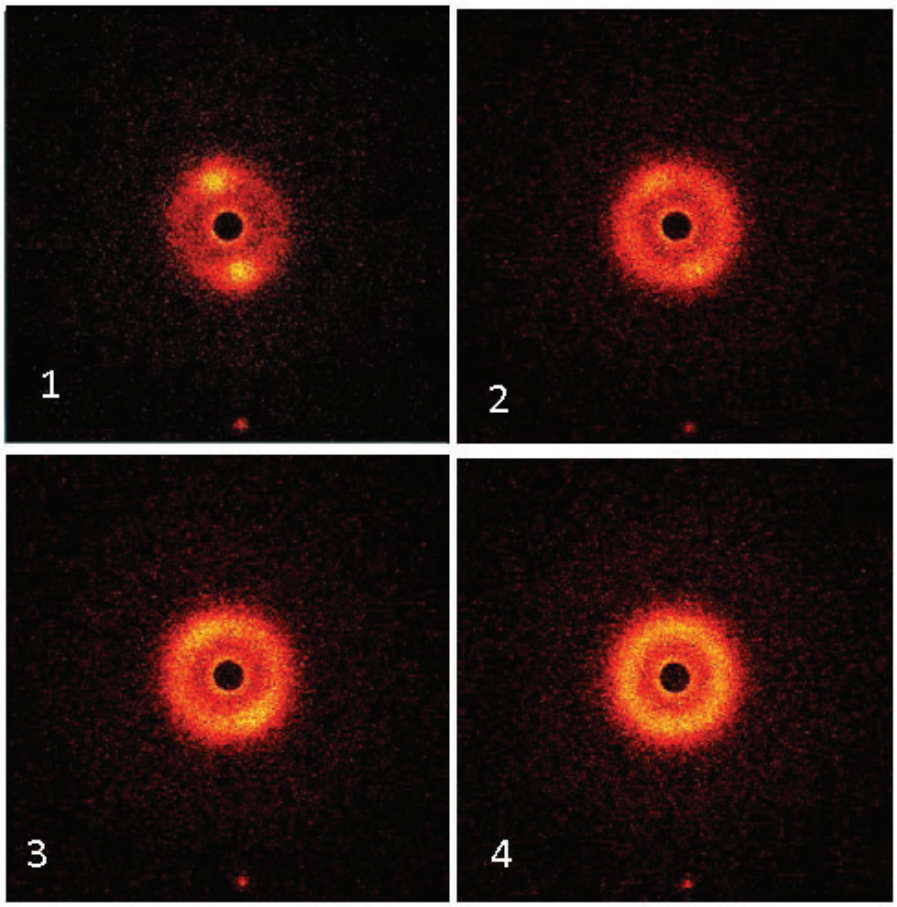

Fig 8: False colour images of the SAXS recorded for samples MM1, MM2, MM3 and MM4. In all cases the long axis of the moulded part was mounted so that it was vertical on this page of images The Q range of the image is (-0.2 to +0.2) Å-1

For each moulded part we measured 2d SAXS patterns and those for MM1 to MM4 are shown in Figure 8 and those for MM5 to MM8 are shown in Figure 13. The SAXS patterns shown in Figure 8 are typical for a semi-crystalline polymer such as poly(e-caprolactone). The peak(s) arise from the lamellar chain folded crystals which form in long-chain polymers. Figure 9 shows cross sections through the intensity map for MM1 and the peak maxima is located at Q=0.042Å^{-1}. The fact that the height of the peak in the vertical and horizontal sections is different reflects the anisotropic nature of the scattering as can clearly be seen in Figure 8. The fact that the pattern is most intense on the vertical sections allows us to determine that the chain folded lamellar crystals are arranged so that the large plane of the crystal is normal to the vertical axis. As the polymer chains will more or less be normal to the lamellar surfaces that the c-axis of the crystals is also parallel to the vertical axis.

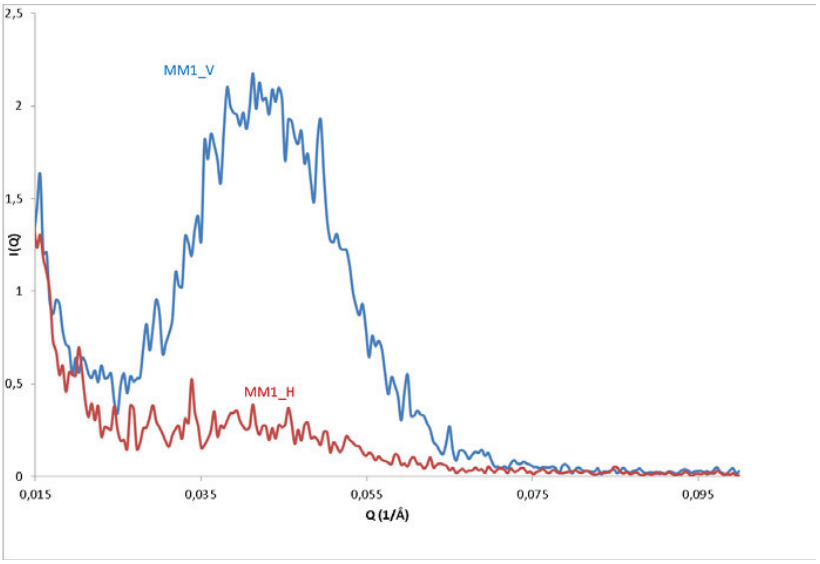

Fig 9: Plots of the horizontal(red line) and vertical (blue line) sections of the SAXS pattern for sample MM1. In Each case the section is taken at Q=0Å^{-1}

We can see the level of anisotropy by taking an azimuthal section centred on the peak maximum at Q=0.042Å^{-1}. This section is shown in Figure 10. We can use these data to calculate an orientation parameter $\langle P_2 \rangle$ for the preferred orientation of the lamellar crystals. A value of $\langle P_2 \rangle$=0 corresponds to an isotropic distribution, whereas a value of 1 corresponds to a uniform orientation with respect to the symmetry axis. The methodology for this is described in references [6-8]. We have extracted the azimuthal profile for each of the SAXS patterns, those for MM2-MM4 are shown in Figure 11, while the curves for MM5to MM8 are largely isotropic and are not shown here. We have obtained the $\langle P_2 \rangle$ values for each which are plotted in Figure 12.

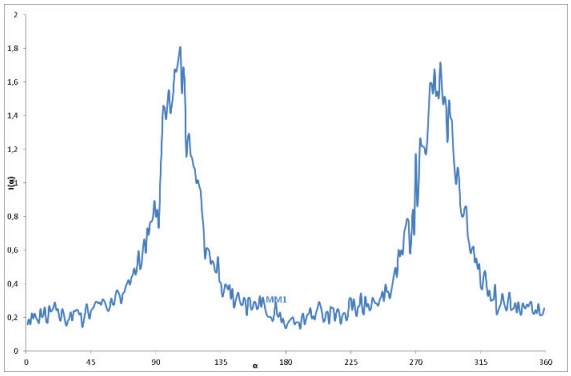

Fig 10: Plot of the intensity I(α) at Q=0.042Å-1 for the SAXS pattern for sample MM1.

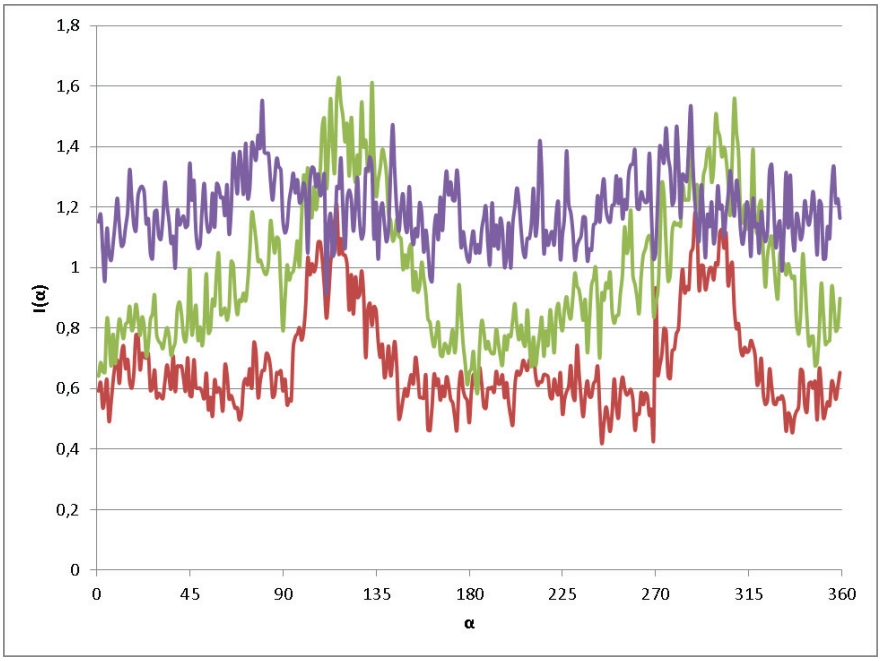

Fig 11 Plot of the azimthual intensity I(α) at Q=0.042Å-1 for the SAXS pattern for sample MM2, MM3 and MM4.

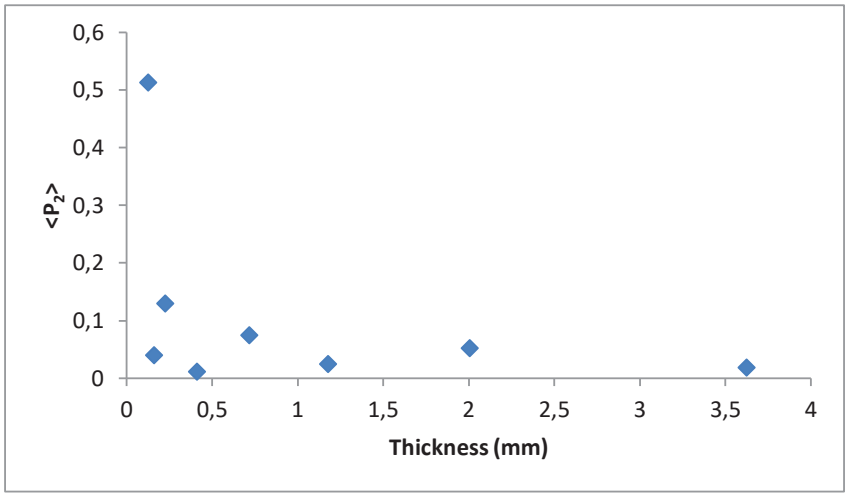

Fig 12: The preferred orientation parameter <P2> obtained for each micromoulded part plotted against the thickness of the micromoulded part.

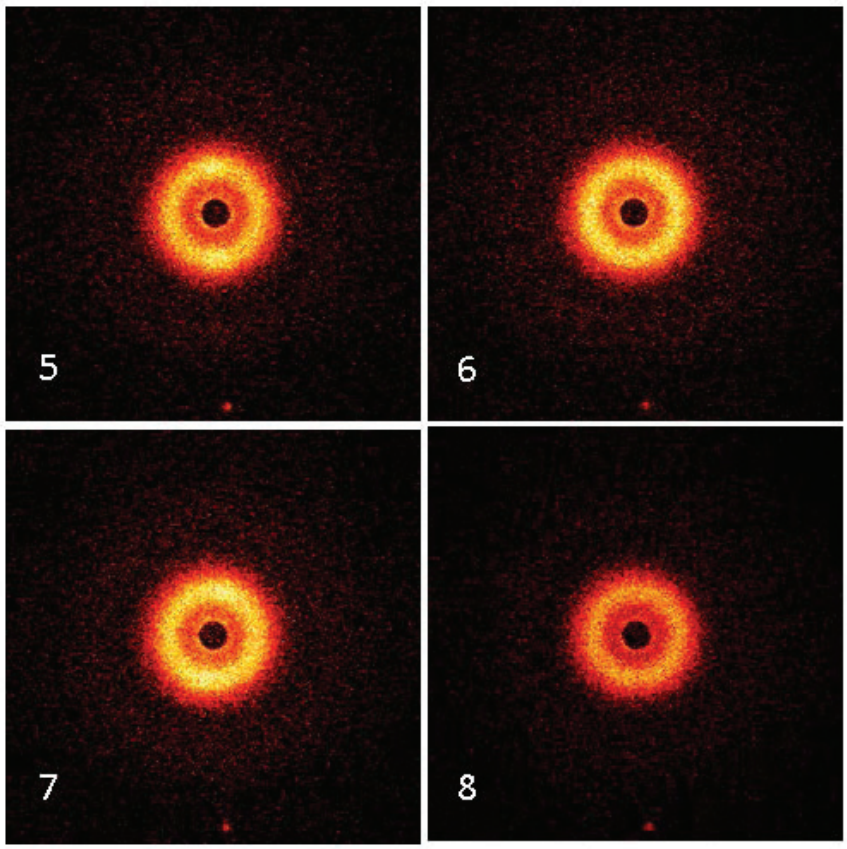

Fig 13: False colour images of the SAXS recorded for samples MM5, MM5, MM7 and MM8. In all cases the long axis of the moulded part was mounted so that it was vertical on this page of images The Q range of the image is (-0.2 to +0.2) Å-1

Conclusions

We show that the thickness of the moulded part produced by microinjection moulding has a major impact on the structure and morphology of that moulded part. When the thickness is small, in our work less than 150μm, the accompanying rapid cooling leads to a high common alignment of the chain folded crystals which form. This is due to the fact that crystallization is initiated prior to the relaxation of the row nuclei formed in the injection phase of the moulding process. For parts with a thicknesess greater than 0.5mm, the semi-crystalline structure is completely isotropic. At intermediate thickness, the parts appear to exhibit a skin/core morphology reported by others. This work was performed using poly(ε-caprolactone) which is biodegradable polymer widely used in medical devices, an area of particular application of micro injection moulding. The morphology has a particular impact on the rate of hydrolytic degradation as it affects direct the diffusion of fluids in to the PCl samples through the amorphous parts.

Acknowledgements

This work was performed as part of the UC4EP (Understanding Crystallisation for Enhanced Polymer Properties) at CDRSP P2020-PTDC/CTM-POL/7133/2014 Funded by FCT. The x-ray scattering measurements were performed in the Chemical Analysis Facility at the University of Reading.

References

[1] M. Heckele, W.K. Schomburg 2004 Review on Micromolding of Thermoplastic Polymers, Journal of Micromechanics and Microengineering, 14 (3) , 1–14
[2] J. Giboz, T. Copponnex, P. Mélé 2007 Microinjection Molding of Thermoplastic Polymers: A Review
Journal of Micromechanics and Microengineering, 17 (6) 96–109
[3] M.T. Martyn, B.W. Whiteside, P.D. Coates, P. Allen, G. Greenway, P. Hornsby Aspects of Micromolding Polymers for Medical Applications Annual Technical Conference (ANTEC) of the Society of Plastics Engineers (SPE), Chicago (2004)
[4] J.Giboz, T.Copponnex and P.Mele 2009 J. Micromech. Microeng. 19 025023
[5] D.Yao in Chapter 7 "Micromolding of Polymers" in Advances in Polymer Processing Woodhead Publishing 2009 552-578
[6] G.R.Mitchell and Ana Tojeira editors 2016 "Controlling Controlling the Morphology of Polymers: Multiple Scales of Structure and Processing." Springer ISBN 978-3-319-39320-9 Springer:Switzerland
[7] B. Gupta, Geeta, A.R. Ray, Preparation of Poly(e-caprolactone)/Poly(e-caprolactone-co-lactide) (PCL/PLCL) Blend Filament by Melt Spinning, Journal of Applied Polymer Science 123 (2011) 1944 - 1950
[7] G.R.Mitchell 2018 "Scattering Methods for Polymer Orientation Characterisation" Springer
[8] R.Lovell and G.R.Mitchell 1981 Molecular Orientation Distribution Derived from an Arbitary Refelection Acta Cryst A37 135-137